WIND PROFILE CONSTANTS IN A NEUTRAL ATMOSPHERIC BOUNDARY LAYER OVER COMPLEX TERRAIN

WILLIAM P. KUSTAS and WILFRIED BRUTSAERT

School of Civil and Environmental Engineering, Cornell University, Ithaca, NY 14853, U.S.A.

(Received in final form 19 March, 1985)

Abstract. The roughness height z_0 and the zero-plane displacement height d_0 were determined for a region of complex terrain in the Pre-Alps of Switzerland. This region is characterized by hills of the order of 100 m above the valley elevations, and by distances between ridges of the order of 1 km; it lies about 20 to 30 km north from the Alps. The experimental data were obtained from radiosonde observations under near neutral conditions. The analysis was based on the assumption of a logarithmic profile for the mean horizontal wind existing over one half of the boundary layer. The resulting (z_0/h) and (d_0/h) (where h is the mean height of the obstacles) were found to be in reasonable agreement with available relationships in terms of placement density and shape factor of the obstacles, which were obtained in previous experiments with h-scales 2 to 4 orders of magnitude smaller than the present ones.

1. Introduction

In various fields dealing with the human environment, the need arises to parameterize the mean wind speed profile and the turbulent momentum transfer in the atmosphere near the earth's surface. This is commonly done within the framework of boundary layer similarity theory. However, most of the work in the past has been done over relatively flat and even surfaces, and very little information is available for complex and rugged hilly terrain. In this paper, an investigation is presented of the applicability of similarity concepts for the atmospheric boundary layer (ABL) over such complex terrain under neutral conditions. The main objective is to determine the surface parameters, namely the roughness height z_0 and the displacement height d_0, in order to allow the estimation of the regional value of the surface shear stress, as expressed in the friction velocity u_*. The rationale of investigating nearly adiabatic conditions is that buoyancy effects due to density stratification can be neglected; thus the similarity formulations are in their simplest form, and the surface parameters, which are in fact also needed for non-neutral conditions, can be obtained much more easily. The analysis makes use of measurements, which were taken during a field program conducted from May through August, 1982, at the Rietholzbach watershed, Switzerland, within the context of ALPEX.

2. The Experiment

2.1. Physical description of the region

The Rietholzbach watershed, with an area of 3.18 km^2, is situated in the Canton St. Gall in the eastern part of Switzerland (approximately 9° E, 47°23′ N), where it crosses the boundaries of Mosnang and Kirchberg. The area surrounding the catchment lies within

Boundary Layer Meteorology **34** (1986) 35–54.

the region generally referred to as Pre-Alps ('Voralpen'); it is characterized by hills of the order of 10^2 m above the valley elevations, which are normally between 600 and 800 m above mean sea level. This Pre-Alpine region is quite rough, with distances between major hill peaks about 1 km and steep side slopes. Approximately 10 km south and southwest of the watershed there are several peaks that extend significantly (about 300 m) above the surrounding valleys; about 10 km east and northeast the hills diminish in size and concentration, to about 1/2 to 2/3 the values near the catchment. However, except for these two discrepancies, the terrain features within a radius of approximately 15 to 20 km are such that for a given wind direction, the regional terrain can probably be treated as statistically uniform. Approximately 20 km to the south of the Rietholzbach lies the edge of the Alpine region. Clearly, the proximity of this high mountain range, running essentially east-west, should have a strong effect on the planetary boundary layer for certain wind directions.

2.2. Radiosonde measurements

Profiles of mean wind speed, temperature and relative humidity in the boundary layer were determined by means of the Thommen radiosonde. The reliability of this sonde has been evaluated in the inter-comparison test, SONDEX, with 11 other types of radiosondes (Richner and Phillips, 1982). Intensive observations were conducted from late May through August, with a total of 300 sondes released during the period. Detailed information on the schedule of the ascents and the data is given elsewhere (Grebner and Brutsaert, 1984). Signals at regular time intervals from the sonde gave values of pressure (p), temperature (T), relative humidity (u) every 30 s, or approximately every 100 to 150 m in the boundary layer, depending on the ascent rate of the balloon. Level 0, with values of p, T, and u was recorded 5 s after sonde release; 30 s later the values of level 1 were acquired, then 1 min of flight later the data of level 2 were recorded, and so on. The position of the sonde in terms of azimuth and elevation angles relative to the launch site was given every 60 s, i.e., on every even-numbered level. Except for a few cases, almost all of the 300 ascents provided profiles to a height of 500 mb, i.e., approximately 5 to 6 km above sea level.

2.3. Neutral boundary-layer data

Neutral conditions are rare occurrences. Therefore, out of 300 ascents only 12 were judged to be sufficiently close to neutral and reliable for wind profile analysis. For each of the 12 flights, the calculated values of height, wind velocity, wind direction and virtual potential temperature at the levels in the boundary layer and one point above it are given in Table I. For all flights, except flight 286, the height of the boundary layer is taken at the inversion in the θ_v profiles. For flight 286, which does not exhibit any inversion below 2000 m, level 6 was estimated as the ABL height, as this corresponds approximately to the Ekman layer thickness $0.3u_*/|f|$. The average depth of the ABL is approximately 830 m with a standard deviation of 245 m.

Four criteria, which are listed in Table II, were employed to ascertain the neutrality of the 12 flights. From the first column it can be seen that the Obukhov length $|L|$ is

TABLE I

Calculated wind speed and virtual potential temperatures profiles

Level	Height z (m above release point)	Wind velocity V (m s^{-1})	Wind vector direction (clockwise from North in deg)	Virtual potential temperature θ_v (K)
FLIGHT 62				
0	9			297.7
1	139	6.1	81	297.4
2	279			297.1
3	469	9.9	83	297.5
4	555			297.6
5	730	10.2	83	297.1
6	907			297.0
7	1016	18.4	73	297.3
8	1208			297.7
9	1352	13.3	81	298.2
FLIGHT 260				
0	9			305.6
1	180	7.0	72	305.0
2	362			305.3
3	459	8.8	55	304.9
4	646			305.2
5	776	10.5	75	305.7
6	968			306.4
FLIGHT 268				
0	27			296.8
1	129	4.0	49	296.9
2	221			296.8
3	380	5.6	56	297.0
4	532			296.8
5	705	6.7	66	296.8
6	842			297.2
7	1071	9.5	73	298.6
FLIGHT 278				
0	28			301.5
1	140	7.3	69	300.9
2	244			301.1
3	377	9.3	70	300.8
4	541			301.3
5	677	11.2	73	301.2
6	856			301.8
7	966	13.7	74	301.6
8	1139			302.3
FLIGHT 283				
0	18			288.3
1	125	2.4	136	290.0
2	225			290.3
3	316	3.7	50	290.3

Table I (continued)

Level	Height z (m above release point)	Wind velocity V (m s^{-1})	Wind vector direction (clockwise from North in deg)	Virtual potential temperature θ_v (K)
FLIGHT 283 (cont.)				
4	409			290.4
5	530	1.7	82	291.1
6	615			291.4
FLIGHT 286				
0	18			295.9
1	110	3.1	155	295.8
2	304			295.6
3	493	4.7	142	295.5
4	674			295.3
5	878	4.5	93	295.3
6	1086			295.2
7	1267	3.9	81	295.3
8	1440			295.4
9	1565	4.8	55	295.4
FLIGHT 96				
0	46			296.6
1	183	3.9	52	296.2
2	350			296.1
3	519	5.3	90	296.0
4	662			296.0
5	836	8.2	91	296.0
6	973			296.8
FLIGHT 97				
0	55			299.3
1	185	3.6	41	298.5
2	344			298.4
3	457	4.9	74	297.9
4	600			298.0
5	774	6.7	70	297.8
6	901			297.7
7	1070	7.9	80	298.1
8	1201			298.2
9	1313	11.4	69	298.5
FLIGHT 184				
0	18			294.7
1	109	2.2	220	294.6
2	201			294.6
3	350	3.1	238	295.0
4	435			294.8
5	577	3.3	244	294.9
6	682			295.1
7	858	3.9	283	296.3

Table I (continued)

Level	Height z (m above release point)	Wind velocity V (m s^{-1})	Wind vector direction (clockwise from North in deg)	Virtual potential temperature θ_v (K)
FLIGHT 197				
0	18			299.3
1	111	2.4	248	299.3
2	252			299.4
3	385	3.6	251	299.5
4	519			299.6
5	645	3.5	274	299.8
6	724			300.5
FLIGHT 223				
0	9			296.0
1	110	2.1	87	295.7
2	231			295.6
3	353	3.6	80	296.1
4	428			295.9
5	533	4.7	81	296.5
6	620			296.3
7	736	4.9	83	297.1
FLIGHT 236				
0	9			300.8
1	167	2.5	143	300.7
2	280			300.7
3	413	3.6	137	300.7
4	548			300.9
5	693	3.0	118	300.6
6	811			301.0
7	971	3.4	93	301.6

equal to or exceeds 10^2 m for seven ascents implying near-neutral conditions, while for the remaining five, the L-values indicate some instability. L is defined as

$$L = \frac{-u_*^3 \rho}{kg\,[(H/c_pT) + 0.61E]}$$

where H the sensible heat flux, and E, the latent heat flux, were determined at a micrometeorological station near the sonde release site, and u_* was determined from the mean wind speed profiles (see Table IV). The other symbols are ρ the density of the air near the ground, T the air temperature, c_p the specific heat at constant pressure, g the acceleration of gravity and k von Karman's constant.

In the second column, the lapse rate of the mean virtual potential temperature θ_v was obtained by taking the change in θ_v between levels 0 and 1. This column indicates that most ascents measured nearly adiabatic profiles; exceptions are flights 97 and 278, which seem to be unstable, and 283, which exhibits stable stratification near the ground.

TABLE II

Criteria used to determine neutrality in the 12 ascents

Ascent No.	Obukhov length L (m)	Lowest level $d\theta_v/d_z$ (K 100 m^{-1})	Pasquill stability class	General weather conditions
62	− 582	− 0.26	D	Mostly cloudy, strong winds
260	− 287	− 0.33	C	Clear skies, strong winds
268	+ 290	+ 0.11	D	Mostly cloudy, moderate winds
278	− 278	− 0.62	D	Scattered clouds, strong winds
283	− 96	+ 1.60	D	Morning: light winds
286	− 98	− 0.05	C-D	Partly cloudy, cool, moderate winds
96	− 36	− 0.30	C	Mostly sunny, precipitation several hours before flight, moderate winds
97	− 220	− 0.62	D	Partly cloudy, moderate winds
184	− 9	− 0.10	C-D	Mostly overcast, light winds
197	− 35	− 0.02	B	Clear skies, light winds
223	− 42	− 0.25	C-D	Overcast, light winds
236	− 81	− 0.03	B-C	Scattered clouds, light winds

B – moderately unstable conditions
C – slightly unstable conditions
D – neutral conditions

The stability classes shown in the third column are Pasquill's (1961); the data required for this classification are wind speed near the ground and insolation. Pasquill's (1961) classification scheme was developed on the basis of experimental data over terrain which was not as rugged as that of the present study. To adapt the wind speed classes to the Rietholzbach region, it was assumed that Pasquill's experiments had a typical roughness of z = 1 cm and a wind measurement height of 10 m; in the present case, z_0 is of the order of 4 m (see below) and the height of the wind speed used was of the order of 10^2 m. Thus, if u_R is the wind speed at the Rietholzbach site, and u_P that in Pasquill's scheme, with (1) one obtains the ratio $u_R/u_P = \ln(100/4)/\ln(10/0.01) = 0.47$. In other words, under similar conditions of insolation, the winds in the Pre-Alpine region at 100 m height can be approximately 50% lower than those defining Pasquill's classes and still result in the same stability class. The third column shows that only two cases deviate moderately from neutral, viz., flights 197 and 236. Finally, the fourth column is presented to provide assistance in interpreting how well column 3 actually describes the stability of each ascent.

Inspection and comparison of all four criteria for each ascent in Table II suggest that the ascents should be subdivided into two groups. The first six ascents (as listed in Tables I and II) appear to satisfy most of the criteria for neutrality fairly well. Those in the second group of six appear to be slightly unstable, but each still has one or other

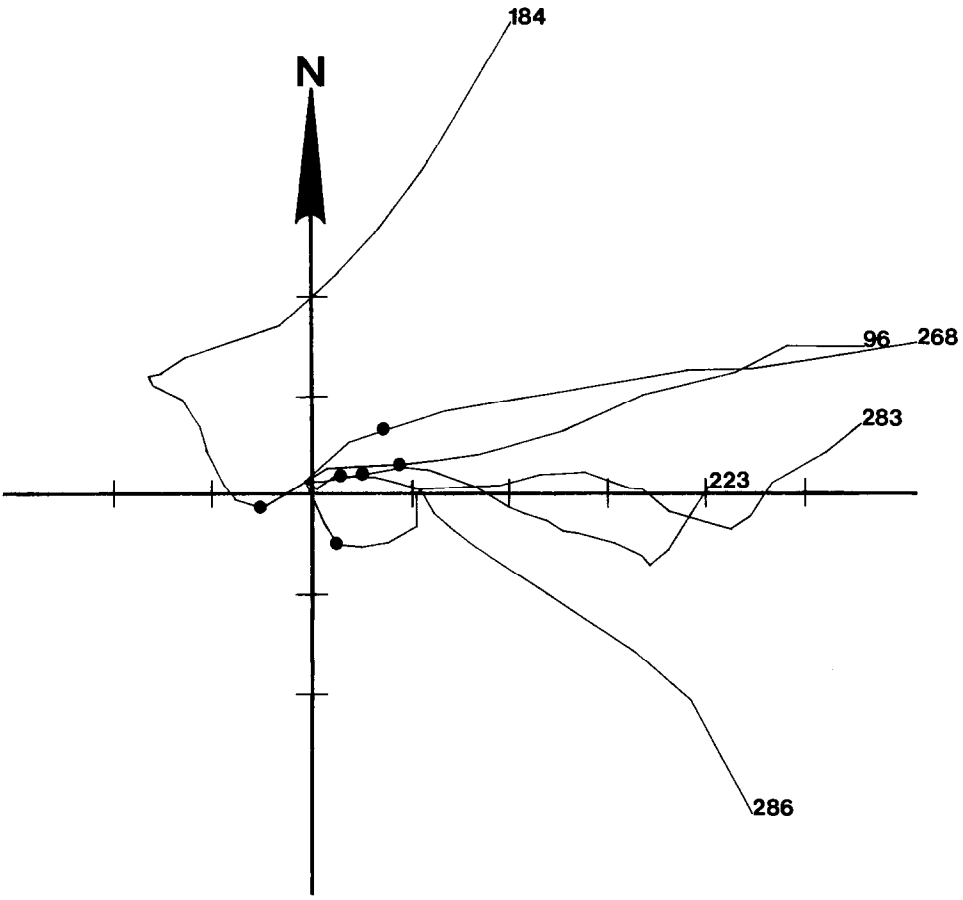

Fig. 1. Horizontal projection of path of sonde for each ascent indicating the wind direction. The solid circle through each path defines the upper limit of the ABL, and the position of the antenna is at the center of the cross. The distance between tick marks along the axes equals 1 km.

feature which could qualify it as close to neutral in some respect, so that it should be considered further. In what follows, therefore, the two groups will be analyzed separately, and subsequently tested to determine whether the two separate estimates of the roughness parameters are statistically different.

Figure 1 illustrates the wind directions for these neutral flights by showing, as examples, the path of the sonde for six ascents, i.e., three from each of the two groups. All of them have the synoptic wind coming from the general westerly direction. It can be seen, however, that among these 6 cases there is both positive (clockwise) and negative (counterclockwise) turning of the wind with altitude within the boundary layer.

3. Review of Previous Work

3.1. Similarity formulations for even terrain

In the lowest regions of the boundary layer in neutral conditions, the wind profile is generally accepted to be logarithmic, viz.

$$\bar{u} = \frac{u_*}{k} \ln\left(\frac{z - d_0}{z_0}\right) \tag{1}$$

where $\bar{u} = \bar{u}(z)$ is the mean wind speed, which is in the direction of the surface shear stress τ_0, z the height above the ground surface, k (= 0.4) von Karman's constant, z_0 the roughness height, d_0 the displacement height, and $u_* = (\tau_0/\rho)^{12}$ the friction velocity, in which ρ is the density of the air. The vertical extent of the validity of (1) is fairly well established for the turbulent boundary layer along a flat plate in a wind tunnel. Such laboratory experiments reported by Clauser (1956) and Hinze (1959) have shown that the region of validity of (1) occupies approximately the lower 10% of the turbulent boundary-layer thickness, that is the so-called inner region. Nevertheless, for laboratory type boundary layers even in the outer region the difference between (1) and the observed profiles is not very large. This was pointed out by Hinze (1959; p. 473) and a similar opinion was voiced by Monin and Yaglom (1971; pp. 300–301; pp. 315–317).

However, this consensus applies only to laboratory flows. For the atmosphere, most of the available information on similarity in the outer region relates not to the wind profile, but merely to the form of the drag coefficient.

In many studies, following the early work of Kazanski and Monin (1961), Csanady (1967), Blackadar and Tennekes (1968) and others, the wind velocity at the top of the boundary layer was assumed to be the geostrophic wind G, as calculated from the pressure gradient; and the thickness of the ABL was assumed to be proportional to u_*/f. But the winds aloft are rarely the result of a balance between the pressure gradient and the Coriolis effect alone over a uniform surface. In fact, the Coriolis effect may be relatively minor compared to the other factors that drive the ABL. Therefore, as suggested by the findings of Zilitinkevich and Deardorff (1974), and Melgarejo and Deardorff (1974, 1975), the use of actually measured values of the wind velocity $V_\delta = (\bar{u}_\delta^2 + \bar{v}_\delta^2)^{1/2}$ and of the ABL height δ, may be more realistic. The drag coefficient, u_*^2/V_δ^2, can be estimated from

$$\bar{u}_\delta = \frac{u_*}{k}\left[\ln\left(\frac{\delta}{z_0}\right) - B\right] \tag{2}$$

and

$$\bar{v}_\delta = -\frac{u_*}{k}A \tag{3}$$

where $\bar{u}_\delta$ is the mean wind component in the direction of u_* and $\bar{v}_\delta$ in the direction normal to it. The minus sign in (3) indicates that $\bar{v}_\delta$ usually points to the right of $\bar{u}_\delta$ in the northern

hemisphere. The parameters A and B in (2) and (3) are constants only under ideal conditions, and even for neutral conditions, they have been found to be quite variable. Several complicating factors have been dealt with in the literature. For example, the results of Johnson (1962), Mendenhall (1967), Arya and Wyngaard (1975), Kondo (1977) and others show that the baroclinity can seriously affect A and B with the possibility of negative (i.e., v_δ to the left of u_δ in the northern hemisphere) values of the turning between u_* and V_δ. The effect of the slope of the terrain was considered from the theoretical point of view by Gutman and Melgarejo (1981) and Sorbjan (1983). It is also generally accepted that A and B should depend on the non-steadiness of the flow, and on horizontal changes in the velocity field (e.g., Hasse, 1976 and Yordanov, 1980). Finally, although this may appear incongruous with the similarity on which (2) through (3) are based, Brown (1982) has raised the possibility that the roughness z_0 of the surface may affect the magnitude of B. Beside the above factors, the complexity of the terrain with valleys, ridges and peaks, can also be expected to make its contribution to channeling of the air flow in the boundary layer in a direction different from those imposed by the Ekman spiral.

3.2. Experimental studies over complex terrain

There have been few investigations dealing with the wind profile over complex hilly terrain, and particularly its roughness at the regional scale. One study, reported by Nappo (1977), was conducted in Eastern Tennessee. Thompson (1978) analyzed rawinsonde data from the Clinch River valley in Carbo, Virginia, while Noilhan *et al.* (1982) conducted a radiosonde experiment in southern France, about 30 km north of the Pyrenees. In the first two of these studies, the wind profile was simply assumed to be logarithmic, to determine the roughness height. In the last one, in which the turning of the wind was considered, the wind velocity at the top of the ABL was assumed to be given by (2) and (3); these drag coefficient equations, rather than the wind profiles, were used to derive z_0 on the basis of data with positive turning; and the data with negative turning were discarded.

3.3. Roughness parameters estimated from surface features

Some empirical equations have been proposed in the past, relating z_0 and d_0 in (1) to simple geometric features of the surface.

(i) The surface roughness height, z_0, is often assumed to be proportional to the mean height, h, of the roughness obstacles as follows

$$z_0 = c_r h \tag{4}$$

with c_r as a constant; Paeschke (1937) obtained $c_r = 1/7.5$, and similar values close to 10^{-1} have been found by many others, especially for surfaces with dense or vegetational roughnesses. The value of c_r actually is quite variable and the following was proposed by Lettau (1969)

$$(z_0/h) = c_s \lambda \tag{5}$$

where c_s is a constant, and $\lambda = (S_n/S_a)$ the roughness density, in which S_n is the silhouette area of the average obstacle, i.e., the area transverse to the wind direction, and S_a is the specific or lot area taken up by the average individual obstacle; put differently, $S_a = A_a/n$, where A_a is the total area occupied by n roughness obstacles. Lettau (1969) proposed $c_s = 0.5$. However, c_s still appears to exhibit some variability, depending on the shape of the roughness elements (e.g., Kondo, 1971; Arya, 1975, Figure 6; Seginer, 1974; Raupach *et al.*, 1980). In the last two studies it was found that for larger values of λ, (z_0/h) decreases with increasing λ. Wooding *et al.* (1973) considered c_s as a shape factor, and from an analysis of numerous data sets for $k = 0.35$ they found

$$c_s = 2.05(h/s)^{0.4} \tag{6}$$

where s represents the streamwise (i.e., horizontal, parallel to the flow) dimension of the roughness elements. If von Karman's constant is given the more classical value of $k = 0.4$, one can adjust the result of Wooding *et al.* (1973), to obtain for the roughness height

$$(z_0/h) = \lambda(h/s)^{0.4} \tag{7}$$

valid over the range $30 < (\delta/z_0) < 2000$. As mentioned above, in the Pre-Alpine region around the Rietholzbach basin, the distances between the hill crests are of the order of 1 km (see Table III); s can be assumed to be about half the value of this wavelength. The average height of the major obstacles in the region is about 95 m. Inserting these values in (7), one obtains $c_s = 0.51$, which is in close agreement with Lettau's value.

Over irregular terrain, (5) has been used by replacing the areal placement density λ by some kind of one-dimensional streamwise density λ_s. Smith and Carson (1977) applied (5) with $c_s = 0.4$, and by defining λ_s as twice the ratio of the average height between peaks and valleys and the average distance between these peaks. Thompson (1978) calculated the density λ_s for several parallel lines drawn in the direction of the

TABLE III

Some terrain features of the region to the west of the Rietholzbach Basin

	Southwest line	Center line	Northwest line	Average
Density, λ_s	0.115	0.078	0.085	0.093
Average Obstacle Height, h (m)	122	82	80	95
Average Height of Valleys Above MSL, $z = 0$ (m)	751	778	743	757
Standard Deviation of Valley Elevations (m)	46.1	65.0	40.3	–
Distances Between Ridges (m)	984	781	1167	977

wind on a topographic map; the number of contours was counted on the windward slopes on all the lines and this was multiplied by the contour interval and then divided by the total length of all the lines. In what follows, the symbols λ_s and λ are used interchangeably.

(ii) The surface displacement height d_0 has been mostly determined for vegetated surfaces; the data appear to be relatively insensitive to density, and it has been suggested that

$$d_0 = c_d h \tag{8}$$

where c_d is another constant, which is of the order of 2/3 (e.g., Brutsaert, 1982).

In the case of bluff-rough surfaces, Kutzbach's (1961) study is apparently the only one in which (d_0/h) has been related to the density. Kutzbach gave as the line of best fit for the bushel basket experiments

$$(d_0/h) = c\,\lambda^d \tag{9}$$

where c and d are constants, which were found to be $c = 1.09$ and $d = 0.29$. To the authors' knowledge, this has not been tested with other data. However, the d_0 values obtained by Raupach *et al.* (1980) for different λ fall well within the scatter of Kutzbach's data; actually for the range $0.09 < \lambda < 0.18$, for which the d_0 values of Raupach *et al.* (1980) are most reliable, they can be described by (9) with $c = 1.47$ and $d = 0.33$, approximately.

4. Analysis

4.1. Representation of the Wind Profile

As mentioned in Section 3, several commonly occurring factors may conspire to make the observed wind profile quite different from that expected for an Ekman layer. Under neutral conditions, these factors may be baroclinicity, flow non-uniformity, unsteadiness and terrain slope; the complexity of the terrain with ridges and valleys or the proximity of large mountain ranges may add further complications. As illustrated in Figure 1, the present experimental data appear to be affected by at least some of these factors. At present, it would seem a hopeless task to include all these factors in any simple formulation of the wind profile. It was also brought out above, that in laboratory situations the turbulent boundary layer can usually be described over most of its depth with sufficient accuracy by a simple logarithmic equation, especially when the flow outside the boundary layer is also turbulent. Therefore, for the purpose of the present analysis, it was decided to disregard any possible turning or spiraling in the wind profile, and to describe it as follows

$$V = \frac{u_*}{k} \ln\left(\frac{z - d_0}{z_0}\right) \tag{10}$$

where $V = (\bar{u}^2 + \bar{v}^2)^{1/2}$ is the mean wind velocity.

Since (2) and (3) (or their Ekman-layer equivalent) have been used to collate numerous experimental data, it may be of interest to see how (10) can be reconciled with these equations for the boundary-layer drag coefficient. From (2) and (3), the wind speed at $z = \delta$ is given by

$$V_\delta = \frac{u_*}{k}\left\{\left[\ln\left(\frac{\delta - d_0}{z_0}\right) - B\right]^2 + A^2\right\}^{1/2} \tag{11}$$

in which d_0 is introduced for consistency with (10). Hence, the condition, for (11) to reduce to (10) at $z = \delta$, is

$$B = \ln\left(\frac{\delta - d_0}{z_0}\right) - \left\{\left[\ln\left(\frac{\delta - d_0}{z_0}\right)\right]^2 - A^2\right\}^{1/2} \tag{12}$$

where the minus sign is required to have $B = 0$ for $A = 0$. If one takes A predicted by Yamada's (1976) equation for adiabatic conditions, i.e., 3.02, (12) yields $B = 0.96$, which is roughly one half of what Yamada's equation for B predicts. Nevertheless, inspection of Yamada's (1976, Figure 5) data shows that $B = 0.96$ is well within the scatter of the data. This suggests that even at the top of the ABL, (10) is often not an unreasonable substitute for (11).

A second possible procedure, as an alternative to (10), to describe wind profiles in the presence of both positive and negative turning can be deduced from inspection of (2) and (3). Indeed, scatter plots of B as a function of atmospheric stability (e.g., Yamada, 1976, Figure 5; Melgarejo and Deardorff, 1974, Figure 3) seem to go through the origin for neutral conditions. A series expansion of (2) in the neighborhood of $z = \delta$, with $B = 0$, yields then (1); but (1) is also valid in the lower reaches of the ABL. Therefore, it is conceivable that, regardless of the turning, it should be the x-component $\bar{u}$, which is logarithmically related to $(z - d_0)$, rather than the total vector as is assumed in (10). It is one of the objectives of this paper to investigate whether the logarithmic function is more suitable for V or for $\bar{u}$.

4.2. Calculation of z_0 from wind profile data

Both equations for the wind profile, (10) and (1), contain three unknown parameters, viz., z_0, d_0, and u_*. In order to determine them, at least three velocity measurements within the ABL must be available. Level 6 is needed to calculate the velocity at level 5, i.e., V_5. Since more than half of the 12 ascents had level 6 within the ABL, it would seem possible to have three velocity measurements within the ABL at least for these ascents. However, because level 6 was usually close to the θ_v inversion, the wind at this level was likely to be affected by the stable stratification. Consequently, the calculated velocity at level 5 was probably also affected. Therefore it was decided to stay a 'safe' distance, say some 10^2 m at least, below the inversion. This left then only two velocity measurements for the analysis with the logarithmic profile, namely V_1 and V_3, where the subscripts refer to the measurement levels.

Because d_0 is known to affect the profile the least of the three variables, it was decided

to assume that it is proportional to z_0, or

$$d_0 = C_0 z_0. \tag{13}$$

If (4) with Paeschke's constant and (8) are used, one obtains simply $C_0 = 5$. Yet if (5) and (9) are adopted, C_0 is a function of the roughness density; using the constants obtained by Kutzbach (1961) and Lettau (1969), one finds

$$C_0 = 2.18\lambda^{-0.71}. \tag{14}$$

For the present study, the value $c_s = 0.5$ of Lettau in (5) is adopted because it is also the value obtainable by (7) for the Pre-Alpine region around the Rietholzbach; Kutzbach's (9) is adopted because it was obtained from the same experiments that yielded Lettau's estimate of c_s. Nevertheless, if the constants obtainable from the data of Raupach *et al.* (1980), viz., $c_s = 0.7$ (see their Figure 1), $c = 1.47$, $d = 0.33$, were used, (5) and (9) would produce a very similar result, $C_0 = 2.10\lambda^{-0.67}$.

With the value of C_0 determined, substitution of (13) in the windprofile (10) (the method is the same for (1)), yields the following for u_* and z_0

$$u_* = 0.4(V_3 - V_1)/\ln\left(\frac{z_3 - C_0 z_0}{z_1 - C_0 z_0}\right) \tag{15}$$

and

$$z_0 = z_1[\exp(0.4V_1/u_*) + C_0]^{-1} \tag{16}$$

where the subscripts 1 and 3 refer to the velocities and altitudes of level 1 and 3, respectively. Equations (15) and (16) are solved by iteration; an initial value z_0 is assumed in (15) and a first value of u_* is calculated; substitution of this value in (16) produces a second estimate of z_0, and so on. The procedure converges rapidly.

4.3. Determination of density and height of roughness obstacles

In order to apply (13) with (14), the placement density of the roughnesses must be known. For the irregular array of hills in the Pre-Alpine region, the streamwise density λ_s was defined as the sum of the heights of the protuberances on the windward sides per unit length along a line drawn on a topographic map in the direction of the wind. The sum of the protuberances was obtained graphically by taking the heights of the terrain every 250 m (i.e., 1 cm on a 1:25 000 map) and then plotting them on graphs with some vertical exaggeration. Thus all the heights of the protuberances on the windward sides are added up and then divided by the length of the line. A regional estimate is obtained by summing over several lines. The present procedure is similar but less tedious and time-consuming than Thompson's, which involves the counting of large numbers of contours, which are often difficult to identify visually on steep slopes. The majority of the ascents had westerly winds; therefore, the procedure was applied along three lines which were drawn radially from the radiosonde release point, namely one in the westerly direction of length 9.5 km, and the other two, each of length 8.5 km, in directions roughly 29° clockwise and counterclokwise, respectively, from the westerly direction. The latter

two lines will be referred to subsequently as the northwest and the southwest diagonal, respectively. The profiles are shown in Figure 2, without the vertical exaggeration.

5. Results

5.1. Surface features

It can be seen from Table III that the average value of the valley elevations above MSL is close to 760, which happens to be the elevation above MSL at the release point for the radiosondes during the experiment. Figure 2 illustrates that this is a reasonable value. Inspection of this figure for the westerly and southwesterly profiles reveals an area of high ridges with valley heights essentially 20 m, on average, higher than 760 m, nearly 2 km from the boundary of the Rietholzbach catchment; however, in both instances as the air flow approaches the catchment, the valleys gradually descend to the 760 m level. The line from the northwest contains valley levels close to 760 m throughout, except near the Rietholzbach basin, where it traverses the ridges surrounding the watershed. The estimate of the average density, $\lambda_s = 0.093$, may be on the low side; it was derived from profiles with a horizontal resolution of 250 m, so that some intervening sub-grid scale valleys or ridges may have been omitted. But for the purpose of the present paper this is not very crucial. As can be seen below in Table VI, in the analysis of the wind profile

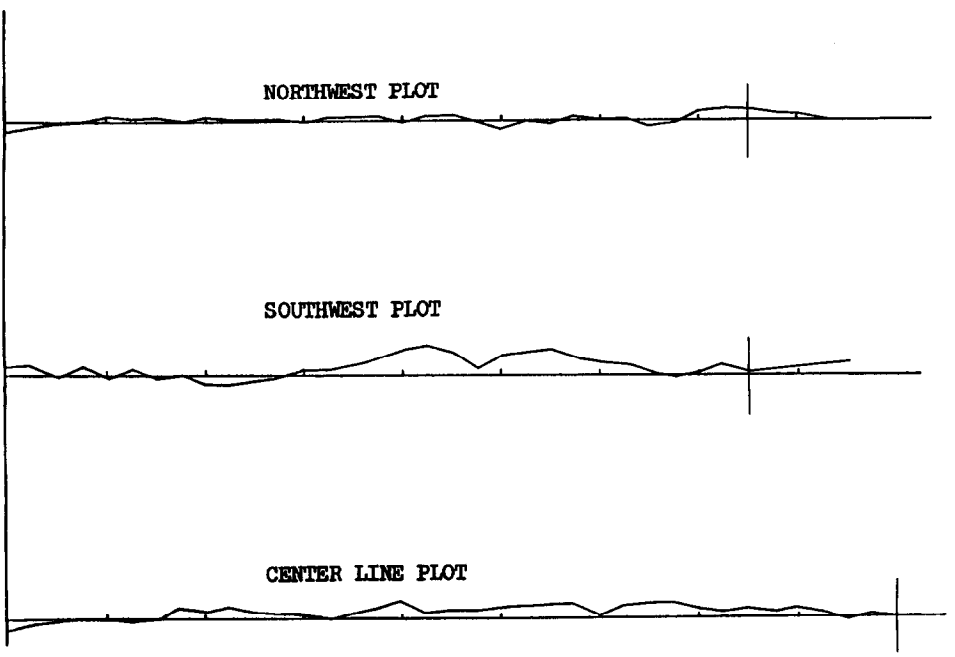

Fig. 2. Plot of the terrain profiles without vertical exaggeration. The reference level is at 760 m above MSL. Vertical bars indicate boundary of Rietholzbach catchment. The distance between tick marks along the abscissa equals 1 km.

data by means of (15), (16), and (14), changes in density as large as 20% produce changes in z_0 and d_0 which are considerably smaller than their respective standard deviations.

5.2. The Roughness Parameters

A first estimate of z_0 and d_0 was made by means of (15) and (16) with C_0 ($= d_0/z_0$) = 5 for both the total wind, V, and the x-component, $\bar{u}$. The results of these calculations, which are not given here, showed that the use of the logarithmic profile for V produces a lower standard deviation, i.e., more consistent results for z_0, than the logarithmic profile for $\bar{u}$; thus from the present data it appears that in the ABL, (10) is preferable over (1). However, the results also indicated that the assumption $d_0 = 5z_0$ is not valid, because it leads to inconsistent results. Indeed, the value $C_0 = 5$ in (13) is derived from the relationships (4) and (8). Yet, the results yielded ratios of (h/z_0) and (h/d_0) which were nearly 60% larger than predicted by (4) and (8). Hence (4) and (8) are oversimplifications for the surface features of the Pre-Alpine Region, and the results obtained with $C_0 = 5$ are invalid.

TABLE IV

Estimates of z_0 and d_0 from wind profile data, by means of (15) and (16) with $C_0 = 12$.

Ascent No.	z_0 (m)	d_0 (m)	u_* (m s^{-1})	u_* (obtained from V_3 with $z_0 = 3.8$ m and $d_0 = 46$ m)
62	3.3	39.4	0.72	0.74
260	2.3	28.0	0.67	0.75
268	3.5	42.3	0.50	0.51
278	2.1	25.2	0.73	0.83
283	5.0	60.4	0.37	0.34
286	2.6	31.7	0.36	0.39
96	4.1	49.1	0.44	0.44
97	5.3	64.2	0.46	0.42
184	2.5	30.2	0.25	0.28
197	3.5	41.6	0.32	0.33
223	4.8	58.2	0.35	0.33
236	5.9	71.1	0.36	0.32
Average	3.8	45.1	0.46	0.47

Table IV shows the results of the computations of z_0, d_0, and u_* by means of (15), and (16) in which C_0 is now allowed to be a function of density as given by (14). The density calculated for the region, $\lambda_s = 0.093$ as given in Table III, produces a value $C_0 = 12$, and this is the value used in the computations. In Table V the means of these z_0 and d_0 estimates are presented separately for the two groups of ascents, and also in combination. In order to test whether the two sets of data actually have values of z_0 which are significantly different from their combined average, a t-test was performed.

TABLE V

Averages of the z_0 and d_0 estimates given in Table IV

	Average z_0 (m)	Standard deviation z_0 (m)	Average d_0 (m)
Group 1 (First 6 ascents of Table II)	3.2	1.1	37.8
Group 2 (Last 6 ascents of Table II)	4.4	1.3	52.4
All 12 ascents combined	3.8	1.3	45.1

Note that the standard deviation of d_0 is C_0 times that of z_0.

For group 1, the calculated t-value for the difference between the sample mean (3.2 m) and the assumed population mean (3.8 m) was 1.49; for group 2, the calculated t-value for the difference between 4.4 and 3.8 m was 1.1. Both calculated t-values are smaller than the t-statistic at the 0.05 significance level, viz. 2.015. This means that the hypothesis that $z_0 = 3.8$ m for both subgroups cannot be rejected at this level. It also means that the combination of the estimates of z_0 and d_0 from both groups is statistically acceptable. Accordingly, the combined estimates will be used in the remainder of the analysis.

To test the sensitivity of the results to the value of the density, the mean results are presented for a range of C_0 between 10 and 15 in Table IV. From the values presented, it is evident that z_0 and d_0 remain practically the same for all C_0 values, or at least within their standard deviations; this substantiates the earlier statement that any possible discrepancies or uncertainty in the roughness density λ, even amounting to 20% or more, are not very significant in the determination of z_0 and d_0 with the present procedure.

Nevertheless, in order to allow the best estimate of z_0 and d_0 with the data, also shown in Table VI in the last row are values of z_0/h as obtained by means of (5) or (7) for the given density λ. Comparison of these values with those obtained from the V-data (in the row just above) shows that $\lambda = 0.073$ produces the most consistent results. In other words, the corresponding value $C_0 = 14$ resulting from (14), produces with (15) and (16) a value of $z_0/h = 0.036$, which is the closest to that obtained by means of (5) on which (14) is based. The same cannot be said for $\lambda = 0.0905$, the value closest to that given in Table III, because the two values of (z_0/h) given under $C_0 = 12$ in Table VI are somewhat different (0.040 and 0.045). Yet, as was pointed out above, the density value of 0.093, obtained from the terrain profiles shown in Figure 2, is likely to be an underestimate, because of the horizontal resolution of these profiles. Hence, $\lambda = 0.073$ is even more likely to be an underestimate. In summary, the results presented here produce two somewhat discrepant findings. On the one hand, Table VI shows that

TABLE VI

Estimates of average z_0 and d_0 from wind profile data, V, by means of (15) and (16) for different assumed values of C_0

C_0	10	11	12	13	14	15
Implied density λ from (14)	0.12	0.10	0.09	0.08	0.07	0.07
Average z_0 (m)	4.2	4.0	3.8	3.6	3.4	3.3
Standard deviation z_0([a])	1.5	1.4	1.3	1.2	1.1	1.1
Average d_0 (= $C_0 \times z_0$)	41.7	43.6	45.1	46.7	48.0	49.3
Average (z_0/h) for h = 95 m	0.044	0.042	0.040	0.038	0.036	0.035
z_0/h estimates from (5) or (7)([a])	0.058	0.051	0.045	0.040	0.036	0.033

([a]) Corresponding values of d_0 are C_0 times those for z_0.

$\lambda = 0.073$ and $C_0 = 14$ yield the best agreement with the value of (z_0/h) obtainable from (5) or (7). On the other hand, with more likely values of the density, (14) suggests that C_0 may be as low as about 10, but not larger than 12. Therefore at this point, it seems reasonable to maintain as a compromise the value $C_0 = 12$, derived from the density λ_s given in Table III.

This discrepancy in density is undoubtedly due to the limitations inherent in the present analysis, which are worth stating. First, there are the limitations of (14) which is based on (5) or (7) and (9); such relationships were obtained statistically by regression analysis from data with considerable scatter. Second, there is the problem of using λ_s instead of λ; this also involves the problem of similarity between, on the one hand, flat surfaces covered with bushel baskets or other regular arrays of identical objects with regular geometry, and on the other hand, a region of non-distinct, non-uniformly sized and randomly arranged roughness obstacles, covered with secondary obstacles such as houses and patches of trees. Third, there is the possibility that a terrain profile over a fetch of 10 km is not long enough to characterize a region. Fourth, one has the assumption that the logarithmic profile (10) is valid over a significant portion of the depth of the ABL. And fifth, there is the limited accuracy of the data given in Table I. In view of all this, the above discrepancy is in fact remarkably small.

Hence, for $C_0 = 12$, the resulting mean values of the roughness parameters can be taken approximately $z_0 = 3.8$ m and $d_0 = (C_0 z_0) = 46$ m. Further support for these values will be given in a subsequent paper dealing with the specific humidity profiles.

The analysis, the results of which are shown in Tables IV and V, was also performed on the x-component of the velocity, $\bar{u}$. However, the standard deviations of z_0 were again larger than those shown in Table VI. Therefore these results are not presented here. Finally, some attempts were made to improve on the data given in Table I by smoothing the observed positions of the radiosonde in the hope that random errors might be reduced. Several techniques were used, which consisted of taking running averages, with various weighting, of the recorded sonde heights H; the velocities $\bar{u}$ and $\bar{v}$ were also recalculated accordingly. However, these techniques all resulted in higher coefficients of variation for the estimates of z_0 and d_0, than those obtained with the actually measured data. This shows that smoothing did not improve the data.

6. Concluding Remarks

The present analysis indicates that the assumption of a logarithmic profile for the mean wind speed, V, over a substantial portion of the depth of the ABL leads to reasonable results in the estimation of the parameters z_0, d_0, and u_*. Further support for the values of u_* obtained here will be given in a later paper by the analysis of the profiles of the mean specific humidity. The mean values of z_0 and d_0 obtained here follow with acceptable fidelity the relationships of these parameters with roughness placement density, obtained in the bushel basket experiments of Kutzbach (1961) and Lettau (1969) and also, but less so, with those in the wind-tunnel experiments of Raupach *et al.* (1980). The results for z_0 are also in agreement with the relationship with density and shape factor obtained from wind-tunnel experiments by Wooding *et al.* (1973) and, to some extent, with the relationship derived from a drag partition concept by Arya (1975). Finally, it was found that the absolute value of the mean wind velocity, V, yields more consistent results with the logarithmic profile equation, than does its x-component, $\bar{u}$.

The generality of these findings is somewhat restricted by the location of the experiment, and the quality and quantity of the rawinsonde data. Because the majority of these near-neutral cases had essentially westerly winds parallel to the Alps, the influence of the terrain on the turning in the wind spiral under neutral conditions cannot be studied for gradient or synoptic winds from any other directions. Also, the poor resolution of the wind profile data precludes any further investigation of the vertical extent of the logarithmic wind profile in the ABL, and a more objective method for determining u_*, z_0, and d_0. Experimental work in rugged natural terrain is difficult and costly so there is a general dearth of information on the applicability of turbulence similarity formulations over such surfaces. The present analysis and results, limited as they may be, should provide some guidance for much needed further research.

Acknowledgments

The authors would like to thank Dr H. Lang and Dr A. Ohmura of the Geographical Institute of the Federal Institute of Technology (ETH), Zurich, Switzerland without whose early coordination and inspiration this study would not have taken place; they are also grateful to Mr D. Grebner of the same Institute, for his leadership and detailed planning of the field experiments, and to Mr H. R. Schneebeli, who was invaluable in the procurement of the radiosonde equipment, and the instruction of the field crew. This research has been supported and financed, in part, by the Division of Atmospheric Sciences of the U.S. National Science Foundation through grant ATM8115713.

References

Arya, S. P. S.: 1975, 'A Drag Partition Theory for Determining the Large Scale Roughness Parameter and Wind Stress on the Artic Pack Ice', *J. Geophys. Res.* **80**, 3447–3454.

Arya, S. P. S. and Wyngaard, J. C.: 1975, 'Effect of Baroclinicity on Wind Profiles and Geostrophic Drag Law for the Convective Boundary Layer', *J. Atmos. Sci.* **32**, 767–778.

Blackadar, A. K. and Tennekes, H.: 1968, 'Asymptotic Similarity in Neutral, Barotropic, Atmospheric Boundary Layers', *J. Atmos. Sci.* **25**, 1015–1020.

Brown, R. A.: 1982, 'On Two-Layer Models and the Similarity Functions for the PBL', *Boundary-Layer Meteorol.* **24**, 451–463.

Brutsaert, W.: 1982, *Evaporation Into the Atmosphere*, D. Reidel Publ. Co., Holland.

Clauser, F. H.: 1956, 'The Turbulent Boundary Layer', *Advances in Applied Mechanics*, Vol. 4, Academic Press, New York.

Csanady, G. T.: 1967, 'On the 'Resistance Law' of a Turbulent Ekman Layer', *J. Atmos. Sci.* **24**, 467–471.

Grebner, D. and Brutsaert, W.: (eds.), 1984, 'The EVAPEX-ALPEX Campaign 1982', Hydrological and Meteorological Studies in the Pre-Alpine Research Basin Rietholzbach, Report of Atmospheric Data, *Zuercher Geographische Schriften* No. 18, Geograph. Instit., ETH, Eidgen. Tech. Hochschule, Zuerich, Switz., 203 pp.

Gutman, L. N. and Melgarejo, J. W.: 1981, 'On the Laws of Geostrophic Drag and Heat Transfer over Slightly Inclined Terrain', *J. Atmos. Sci.* **38**, 1714–1724.

Hasse, L.: 1976, 'A Resistance-Law Hypothesis for the Non-Stationary Advective Planetary Boundary Layer', *Boundary-Layer Meteorol* **10**, 393–407.

Hinze, J. D.: 1959, *Turbulence*, McGraw-Hill, New York.

Johnson, Warren B. Jr.: 1962, 'Climatology of Atmospheric Boundary-Layer Parameters and Energy Dissipation, Derived from Gregg's Aerological Survey of the U.S.', in Studies of the Three-Dimensional Structure of the Planetary Boundary Layer, Final Rept., Dept. of Meteorology, University of Wisconsin, Madison, 125–158.

Kazanski, A. B. and Monin, A. S.: 1961, 'On the Dynamic Interaction between the Atmosphere and the Earth's Surface', *Bull. Izv. Acad. Sci. U.S.S.R. Geophys. Ser.* **5**, (Engl. Edn.), 514–515.

Kondo, J.: 1971, 'Relationship Between Roughness Coefficient and Other Aerodynamic Parameters', *J. Meteorol. Soc. Japan* **49**, 121–124.

Kondo, J.: 1977, 'Geostrophic Drag and the Cross-isobar Angle of the Surface Wind in a Baroclinic Convective Boundary Layer', *J. Meterol. Soc. Japan* **55**, 301–311.

Kutzbach, J.: 1961, 'Investigations of the Modification of Wind Profiles by Artificially Controlled Surface Roughness', in Studies of Three Dimensional Structure of the Planetary Boundary Layer, Annual Rept., Dept. of Meteorology, University of Wisconsin, Madison, pp. 71–113.

Lettau, H.: 1969, 'Note on Aerodynamic Roughness Parameter Estimation on the Basis of Roughness-Element Description', *J. Appl. Meteorol.* **8**, 828–832.

Melgarejo, J. W. and Deardoff, J. W.: 1974, 'Stability Functions for the Boundary-Layer Resistance Laws Based upon Observed Boundary-Layer Heights', *J. Atmos. Sci.* **31**, 1324–1333.

Melgarejo, J. W. and Deardorff, J. W.: 1975, 'Revision to 'Stability Functions for the Boundary-Layer Resistance Laws Based upon Observed Boundary-Layer Heights' ', *J. Atmos. Sci.* **32**, 837–839.

Mendenhall, B. R.: 1967, 'A Statistical Study of Frictional Wind Veering in the Planetary Boundary Layer', M. S. Thesis, Colorado State University, Fort Collins.

Monin, A. S. and Yaglom, A. M.: 1971, *Statistical Fluid Mechanics: Mechanics of Turbulence*, Vol. 1, The MIT Press, Cambridge, Mass.

Nappo, C. J.: 1977, 'Mesoscale Flow over Complex Terrain During Eastern Tennessee Trajectory Experiment (ETTEX)', *J. Appl. Meterol.* **16**, 1186–1196.

Noilhan, J., Benech, B., Druilhet, A., and Dubosclard, G.: 1982, 'Etude Expérimentale de la Couche Limite au-dessus d'un Relief Modéré Proche d'une Chaîne de Montagne', *Boundary-Layer Meteorol.* **24**, 395–414.

Paeschke, W.: 1937, 'Experimentelle Untersuchungen zum Rauhigkeits- und Stabilitätsproblem in der Bodennahen Luftschicht', *Beiträge Z. Phys. d. Freien Atmos.* **24**, 163–189.

Pasquill, F.: 1961, 'The Estimation of the Dispersion of Windborne Material', *Meteorol. Mag.* **90**, 33–49.

Raupach, M. R., Thom, A. S., and Edwards, I.: 1980, 'A Wind-Tunnel Study of Turbulent Flow Close to Regularly Arrayed Rough Surfaces', *Boundary-Layer Meteorol.* **18**, 373–397.

Richner, H. and Phillips, P. D.: 1982, 'The Radiosonde Intercomparison SONDEX Spring 1981, Payerne', *Pure and Appl. Geophys.* (PAGEOPH) **120**, 852–1198.

Seginer, I.: 1974, 'Aerodynamic Roughness of Vegetated Surfaces', *Boundary-Layer Meteorol.* **5**, 383–393.

Smith, F. B. and Carson, D. J.: 1977, 'Some Thoughts on the Specification of the Boundary-Layer Relevant to Numerical Modeling', *Boundary-Layer Meteorol.* **12**, 307–330.

Sorbjan, Z.: 1983, 'Rossby-Number Similarity in the Atmospheric Boundary Layer Over a Slightly Inclined Terrain', *J. Atmos. Sci.* **40**, 718–728.

Thompson, R. S.: 1978, 'Note on the Aerodynamic Roughness Length for Complex Terrain', *J. Appl. Meteorol.* **16**, 1402–1403.

Wooding, R. A., Bradley, E. F., and Marshall, J. K.: 1973, 'Drag Due to Regular Arrays of Roughness Elements of Varying Geometry', *Boundary-Layer Meteorol.* **5**, 285–308.

Yamada, T.: 1976, 'On the Similarity Functions A, B, and C of the Planetary Boundary Layer', *J. Atmos. Sci.* **33**, 781–793.

Yordanov, D.: 1980, 'A Note on the Rossby Similarity of a Non-Stationary Atmospheric Boundary Layer', *Beitr. Phys. Atmos., Contrib. Atmos. Phys.* **53**, 167–197.

Zilitinkevich, S. S. and Deardorff, J. W.: 1974, 'Similarity Theory for the Planetary Boundary Layer of Time-Dependent Height', *J. Atmos. Sci.* **31**, 1449–1452.